Contribution from the Department of Chemistry, University of Glasgow, Glasgow G12 8QQ, U.K., Lehrstuhl für Anorganische Chemie I, Ruhr-Universität Bochum, D-4630 Bochum, Germany, and Anorganische-Chemisches Institut, Universität Heidelberg, D-6900 Heidelberg, Germany

Synthesis and Structural and Spectroscopic Studies of Manganese Complexes of Pendant-Arm Macrocycles Based on 1,4,7-Triazacyclononane: Crystal Structures of the Manganese(II) Complex $[MnLH_3][MnCl_4]$ and of the Mixed-Valence Manganese(II)–Manganese(IV) Hydrogen-Bridged Dimer $[MnLH_3LMn][PF_6]_3$ (LH_3 = *N,N',N''*-Tris[(2*S*)-2-hydroxypropyl]-1,4,7-triazacyclononane) and of the Manganese(IV) Monomer $[MnL'][ClO_4]$ ($L'H_3$ = *N,N',N''*-Tris(2-hydroxyethyl)-1,4,7-triazacyclononane)

Arafa A. Belal,[†] Phalguni Chaudhuri,[‡] Ian Fallis,[†] Louis J. Farrugia,*[,†] Robert Hartung,[‡] Norman M. Macdonald,[†] Bernhard Nuber,[§] Robert D. Peacock,*[,†] Johannes Weiss,[§] and Karl Wieghardt*[,‡]

Received November 2, 1990

The pendant-arm macrocyclic ligand *N,N',N''*-tris[(2*S*)-2-hydroxypropyl]-1,4,7-triazacyclononane (LH_3) forms two types of manganese complexes. A mononuclear Mn(II) complex, $[MnLH_3][MnCl_4]$ (**1**), is formed when the ligand is fully protonated. Under mildly basic conditions, partial deprotonation occurs and the mixed-valence Mn(II), Mn(IV) dimer $[Mn^{II}LH_3LMn^{IV}][PF_6]_3$ (**2**) is produced. The crystal structures of both complexes have been determined: **1** is orthorhombic, space group $P2_12_12_1$, with a = 10.744 (2) Å, b = 14.186 (4) Å, c = 15.603(3) Å, and Z = 4; **2** is rhombohedral, space group $R3$, with a = 10.472 (1) Å, c = 36.637 (7) Å, and Z = 3. A notable feature of the structure of the dimer is that the Mn(II) and Mn(IV) halves have different geometries; the coordination around the Mn(II) is trigonal prismatic while that around Mn(IV) is pseudooctahedral. The absorption and CD spectra, the cyclic voltammetry, and the temperature-dependent paramagnetism of the mixed-valence species are reported. The analogous unmethylated ligand, *N,N',N''*-tris(2-hydroxyethyl)-1,4,7-triazacyclononane ($L'H_3$)) forms a monomeric Mn(IV) complex, $[MnL'][ClO_4]$ (**3**), which has pseudooctahedral geometry. The crystal structure of **3** has also been determined: it is cubic, space group $P2_13$, with a = 14.761 (3) Å and Z = 8. The cations of **3** are arranged in pairs with weak contacts between the alkoxy atoms of one molecule and the methylene hydrogens of the other.

Introduction

The "small" macrocycle 1,4,7-triazacyclononane (tacn) has a rich chemistry.[1] Unlike the more familiar tetraazamacrocycles such as cyclam, tacn is too small to form equatorial complexes with transition-metal ions but must instead coordinate facially, giving "sandwich" complexes[2] such as $[Ni(tacn)_2]^{2+}$ or piano-stool complexes[3] such as $[Mo(tacn)(CO)_3Br]^+$. Tacn is readily derivatized at the nitrogen atoms to give N-alkylated ligands such as *N,N',N''*-trimethyl-tacn[4] and *N,N',N''*-tribenzyl-tacn[5] and somewhat less easily substituted on the ring carbon atoms to give compounds such as (2*R*)-2-methyl-tacn.[6] Tacn has been used to prepare a variety of pendant-arm ligands; the arms include $-CH_2COOH$,[7] $-CH_2CH_2NH_2$,[8] $-CH_2CH_2OH$[9] ($L'H_3$), (2*S*)-$CH_2CH(Me)OH$[10,11] (LH_3), $-CH_2(2\text{-}OHC_6H_5)$,[12] and $-CH_2bpy$.[13,14] The ligands with pendant alcohol groups are particularly interesting because they form complexes in which the OH can remain protonated and act as an alcohol or can deprotonate and so act as an alkoxide. LH_3 has the additional advantage of chirality, which leads to the complexes formed being of a single absolute configuration. Peacock et al. have recently reported[11] the structure of the Co(III) complex with LH_3, which occurs as a hydrogen-bridged dimer $[CoLH_3LCo]^{3+}$. In this paper we present the preparation and structural characterization of two manganese complexes of LH_3—the monomeric Mn(II) complex $[MnLH_3][MnCl_4]$ (**1**) and the mixed-valence dimer $[Mn^{II}LH_3LMn^{IV}][PF_6]_3$ (**2**) (Glasgow)—and of a monomeric Mn(IV) complex of the related ligand $L'H_3$ (Bochum and Heidelberg). A preliminary report of the structure of **2** has been published.[15]

Experimental Section

1,4,7-Triazacyclononane (tacn) was prepared according to published procedures.[16] *N,N',N''*-Tris[(2*S*)-2-hydroxypropyl]triazacyclononane (LH_3) was prepared as the hydrochloride salt from tacn·3HCl and (*S*)-(−)-propylene oxide as previously described.[11] *N,N',N''*-Tris(hydroxyethyl)triazacyclononane was prepared as described by Hancock et al.[9]

Synthesis of $[MnLH_3][MnCl_4]$ (1). To a solution of $MnCl_2·6H_2O$ (0.46 g, 2 mmol) in 10 mL of ethanol was added one of $LH_3·HCl$ (0.34 g, 1 mmol) also in 10 mL of ethanol. Complex **1** slowly precipitated as a white microcrystalline powder. It was recrystallized from aqueous ethanol. During the recrystallization a small amount of the complex was oxidized to $[Mn^{II}LH_3LMn^{IV}]^{3+}$. The chloride salt of the latter complex is soluble in ethanol, however, and pure crystals of **1** were obtained by washing with ethanol. Yield: 78%. Anal. Calcd for $C_{15}H_{33}Cl_4Mn_2N_3O_3$: C, 32.46; H, 5.99; N, 7.57; Cl, 25.25. Found: C, 31.95; H, 5.92; N, 7.24; Cl, 25.21.

Synthesis of $[Mn^{II}LH_3LMn^{IV}][PF_6]_3$ (2). To a solution of $MnCl_2·6H_2O$ (0.23 g, 1 mmol) in 10 mL of water was added a solution of $LH_3·HCl$ (0.34 g, 1 mmol) also in 10 mL of water, and the pH of the solution was adjusted to 8 with NaOH. The solution, which was initially colorless, slowly darkened, becoming deep red after about 12 h. Solid $[NH_4][PF_6]$ was added to the red solution and the precipitated $[PF_6]^-$ salt filtered off and recrystallized from boiling acetonitrile to yield small

[†] University of Glasgow.
[‡] Ruhr-Universität Bochum.
[§] Universität Heidelberg.

(1) Wieghardt, K.; Chaudhuri, P. *Progress in Inorganic Chemistry*; Lippard, S. J., Ed.; Wiley: New York, 1988; Vol. 35, p 329.
(2) Zompa, L. J.; Margulis, T. N. *Inorg. Chim. Acta* **1978**, *28*, L157.
(3) Chaudhuri, P.; Wieghardt, K.; Tsai, Y.-H.; Kruger, C. *Inorg. Chem.* **1982**, *23*, 427.
(4) Wieghardt, K.; Chaudhuri, P.; Weiss, J. *Inorg. Chem.* **1982**, *21*, 3086.
(5) Beissel, T.; Della Vedova, B. S. P. C.; Wieghardt, K.; Boese, R. *Inorg. Chem.* **1990**, *29*, 1736.
(6) Mason, S. F.; Peacock, R. D. *Inorg. Chim. Acta* **1976**, *19*, 75.
(7) Wieghardt, K.; Bossek, U.; Chaudhuri, P.; Herrman, W.; Menke, B. C.; Weiss, J. *Inorg. Chem.* **1982**, *21*, 4308.
(8) Hammershoi, B. A.; Sargeson, A. M. *Inorg. Chem.* **1983**, *22*, 3554.
(9) Sayer, B. A.; Michael, J. P.; Hancock, R. D. *Inorg. Chim. Acta* **1983**, *77*, L63.
(10) Peacock, R. D.; Robb, J. *Inorg. Chim. Acta* **1986**, *121*, L15.
(11) Belal, A. A.; Farrugia, L. J.; Peacock, R. D.; Robb, J. *J. Chem. Soc., Dalton Trans.* **1989**, 931.
(12) Auerbach, U.; Eckert, U.; Wieghardt, K.; Nuber, B.; Weiss, J. *Inorg. Chem.* **1990**, *29*, 938.
(13) Alcock, N. W.; McLaren, F.; Moore, P.; Pike, G. A.; Roe, S. M. *J. Chem. Soc., Chem. Commun.* **1989**, 798.
(14) Ziessel, R.; Lehn, J.-M. *Helv. Chim. Acta* **1990**, *73*, 1149.
(15) Belal, A. A.; Fallis, I.; Farrugia, L. J.; Macdonald, N. M.; Peacock, R. D. *J. Chem. Soc., Chem. Commun.* **1991**, 402.
(16) Searl, G. H.; Geue, R. *J. Aust. J. Chem.* **1984**, *37*, 959.

0020-1669/91/1330-4397$02.50/0

Table I. Crystallographic Data for **1–3**

	1	2	3
chem formula	$C_{15}H_{33}Cl_4Mn_2N_3O_3$	$C_{30}H_{64}F_{18}Mn_2N_6O_6P_3$	$C_{12}H_{24}ClMnN_3O_7$
fw	555.1	1149.6	412.7
space group	$P2_12_12_1$	$R3$	$P2_13$
a, Å	10.744 (2)	10.472 (1)	14.761 (3)
b, Å	14.186 (4)	10.472 (1)	14.761 (3)
c, Å	15.603 (3)	36.637 (7)	14.761 (3)
V, Å^3	2378 (1)	3479 (4)	3216.2
Z	4	3	8
T, C	25	25	22
λ, Å	0.71069	0.71069	0.71069
ρ_{calcd}, g cm^{-3}	1.55	1.65	1.705
μ, cm^{-1}	14.94	7.4	9.54
transm coeff	0.78–1.04	0.76–1.14	0.84–0.92
$R(F_o)$	0.034	0.038	0.056
$R_w(F_o)$	0.039	0.049	0.046

dark red prisms. Yield: 65%. Anal. Calcd for $C_{30}H_{63}F_{18}Mn_2N_6O_6P_3$: C, 31.34; H, 5.61; N, 7.31; P, 8.08. Found: C, 31.26; H, 5.53; N, 7.23; P, 7.98.

Synthesis of [MnL′][ClO$_4$] (3). To a solution of $Mn(ClO_4)_2{\cdot}6H_2O$ (0.72 g; 2.0 mmol) in water (10 mL) was added a 1 mol L^{-1} ethanolic solution of $L'H_3$ (2 mL) and solid $NaClO_4{\cdot}H_2O$ (0.4 g). Dropwise addition of 35% H_2O_2 (2 mL) initiated a color change to deep red. The solution was stirred at 20 °C for 30 min until the evolution of O_2 ceased. The solution was allowed to stand in an open vessel for 2 days after which time deep red crystals suitable for X-ray crystallography had formed. These were collected by filtration, washed with ethanol, and air dried. Yield: 66%. Anal. Calcd for $C_{12}H_{24}N_3O_3MnClO_4$: C, 34.92; H, 5.86; N, 10.18; ClO_4 24.09. Found: C, 34.6; H 5.8; N 10.1; ClO_4, 23.8. **3** can also be prepared as the bromide salt by aerial oxidation of equimolar amounts of "manganese(III) acetate" and $L'H_3$, followed by addition of NaBr.

X-ray Diffraction Studies of 1 and 2. Details of the data collection procedures and structural refinements are given in Table I (Table S1, supplementary material). Data were collected on an Enraf-Nonius CAD4 automated diffractometer with graphite monochromated Mo Kα X-radiation (λ = 0.71069 Å). Unit cell parameters were determined by refinement of the setting angles ($\theta \geq 12°$) of 25 reflections. Standards were measured every 2 h, and no significant variation in intensities was noticed. Lorentz–polarization and absorption/extinction (DIFABS[17]) corrections were also applied.

Systematic absences uniquely determined the chiral space group $P2_12_12_1$ for compound **1**. The structure was solved by direct methods (MITHRIL[18]) and subsequent electron density difference syntheses.

In the case of **2** the initial data collection indicated that the hexagonal cell was R centered. The only chiral rhombohedral space groups are $R3$ and $R32$, which respectively require molecular C_3 or D_3 symmetry for the $[MnLH_3LMn]^{3+}$ unit. Analysis was initiated in $R3$ since this gave a more satisfactory R_{merge} (0.042 for 1610 observations), and this space group was confirmed by successful solution and refinement of the structure. The different coordination geometries of the Mn atoms preclude an ordered structure with D_3 symmetry. The structure was solved by heavy-atom methods (for the Mn atoms) and subsequent electron density difference syntheses.

Refinement was by full-matrix least-squares methods, minimizing the function $\sum w(|F_o| - |F_c|)^2$ with the weighting function $w = [\sigma^2(F_o)]^{-1}$ used and judged satisfactory. $\sigma(F_o)$ was judged from counting statistics. All non-H atoms were allowed anisotropic thermal motion. Hydrogen atoms, apart from the O–H atoms, were included at calculated positions with C–H = 1 Å. The O–H hydrogens (H(1), H(2), and H(3) of **1** and H(1) of **2**) were observed in the difference map. All H atoms were assigned a fixed isotropic thermal parameter of 0.05 Å. The expected S configuration of the chiral carbon atoms was confirmed by refining the inverted configuration, which converged to higher residuals of 0.038 (0.046) for **1** and 0.040 (0.053) for **2**, and also by refinement of η, the coefficient of the anomalous scattering factor,[19] which refined to values of 1.01 (8) and 0.74 (14) for the S configuration of **1** and **2**, respectively. The esd of an observation of unit weight (S) was 1.57 for **1** and 3.52 for **2**. Neutral-atom scattering factors were taken from ref 20 with corrections applied for anomalous scattering. All calculations were carried out on a MicroVAX 3600 computer using the Glasgow GX suite of programs.[21]

X-ray Diffraction Study of 3. Intensities and lattice parameters of a red-brown tetrahedrally shaped crystal were measured on a Syntex R3 diffractometer at ambient temperature using graphite-monochromated Mo Kα radiation. Crystal parameters and additional details of the collection are given in Table I (Table S2, supplementary material). An empirical absorption correction (ψ scans) was carried out. The structure was solved by conventional Patterson and difference Fourier methods and refined with anisotropic thermal parameters for all non-hydrogen atoms. Neutral-atom scattering factors and anomalous dispersion corrections for non-hydrogen atoms were taken from ref 20. All methylene hydrogen atoms were placed at calculated positions with C–H = 0.96 Å and group isotropic temperature factors. The function minimized during full-matrix least-squares refinement[22] was $\sum w(|F_o| - |F_c|)^2$ where $w = 1/\sigma^2(F)$. One of the $[ClO_4]^-$ anions of the two crystallographically independent formula units was found to be disordered. The disorder was successfully modeled.

Magnetic Susceptibility Measurements for 2. The temperature-dependent magnetic susceptibility of a solid sample of **2** was measured[23] in the temperature range 2.0–295 K with a SQUID magnetometer (MPMS, Quantum Design). The sample material was contained in a 4-mm quartz tube. Data were evaluated using the standard software of the instrument and were corrected for the diamagnetic response of the holder. Diamagnetic corrections were applied using Pascal's constants.

Results and Discussion

$[MnLH_3][MnCl_4]$ (**1**) is formed as a white precipitate when 1 mol of LH_3 and 2 mol of $MnCl_2{\cdot}6H_2O$ are mixed in ethanol. When solid **1** is dissolved in water, the solution slowly turns red-brown (the reaction is faster if the pH is raised to ~8 with NaOH) to give a deep red solution from which **2** is precipitated on addition of $[NH_4][PF_6]$. **1** can be recrystallized from aqueous ethanol. Under these conditions there is a little oxidation of **1** to give **2**, but this can be removed by washing with ethanol. From the analysis and color, it was clear that both the anion and cation in **1** contained Mn(II).

The red-brown color (and electronic spectrum) of **2** suggested that at least one of the Mn atoms was in the +3 or +4 oxidation state. The analytical data for **2** suggested that it should be formulated as $[MnLH_3LMn][PF_6]_3$ and so might be isostructural with $[CoLH_3LCo][PF_6]_3$. The structural evidence given below, however, indicates that the cation is a Mn(II), Mn(IV) mixed-valence dimer, $[Mn^{II}LH_3LMn^{IV}]^{3+}$. That one of the two Mn atoms is in the 2+ oxidation state was confirmed by the following experiment. When a solution of **2** in CH_3CN was treated with a few drops of Et_3N and exposed to the air, the color intensified. The final spectrum was identical to that of **2** *but had double the extinction coefficient*. The oxidation states of the dimer were further confirmed by magnetic measurements (vide infra). **3** is formed by H_2O_2 oxidation of an equimolar mixture of $Mn(ClO_4)_2$ and $L'H_3$ or by aerial oxidation of $L'H_3$ and "manganese(III) acetate". Magnetic moment measurements ($\mu_{eff}(298) = 4.1\ \mu_B$) confirmed that **3** is a Mn(IV) complex.

(17) Walker, N.; Stuart, D. *Acta. Crystallogr., Sect. A.: Found. Crystallogr.* **1983**, *A39*, 158.
(18) Gilmore, C. J. *J. Appl. Crystallogr.* **1984**, *17*, 42.
(19) Rodgers, D. *Acta. Crystallogr., Sect. A: Found. Crystallogr.* **1981**, *A37*, 734.
(20) *International Tables for X-Ray Crystallography*; Kynoch: Birmingham, England, 1974; Vol. 4.
(21) Mallinson, P. R.; Muir, K. W. *J. Appl. Crystallogr.* **1985**, *18*, 51.
(22) Full-matrix least-squares refinement was performed with the SHELXTL-PLUS program package by G. M. Sheldrick, University of Gottingen, 1988.
(23) We thank Prof. Dr. A. X. Trautwein and Dipl.-Phys. C. Butzlaff (Medizinische Universität Lübeck) for the susceptibility measurements.

Table II. Final Positional Parameters (Fractional Coordinates) with Esd's in Parentheses and Isotropic Thermal Parameters (Å²) (Equivalent Isotropic Parameters Used for Anisotropic Atoms) for $[MnLH_3][MnCl_4]$ (1)

atom	x/a	y/b	z/c	U_{eq}[a]
Mn(1)	−0.00346 (8)	0.21670 (5)	0.24287 (4)	0.026
Mn(2)	0.49729 (9)	0.49611 (6)	0.37966 (5)	0.036
Cl(1)	0.50742 (17)	0.42690 (11)	0.24553 (9)	0.051
Cl(2)	0.45392 (16)	0.38105 (12)	0.48682 (9)	0.051
Cl(3)	0.33908 (16)	0.61160 (14)	0.38905 (11)	0.060
Cl(4)	0.69384 (15)	0.56216 (12)	0.41264 (11)	0.053
N(1)	−0.0911 (4)	0.3374 (3)	0.3147 (3)	0.031
N(2)	−0.0320 (4)	0.3206 (3)	0.1366 (3)	0.028
N(3)	0.1619 (4)	0.3103 (3)	0.2634 (3)	0.030
O(1)	−0.1863 (3)	0.1618 (3)	0.2681 (2)	0.036
O(2)	0.0493 (3)	0.1366 (3)	0.1303 (2)	0.031
O(3)	0.0973 (3)	0.1434 (3)	0.3442 (2)	0.030
C(1)	−0.1948 (6)	0.2932 (4)	0.3650 (4)	0.040
C(2)	−0.2716 (6)	0.2260 (5)	0.3120 (4)	0.043
C(3)	−0.3573 (6)	0.1690 (5)	0.3675 (5)	0.064
C(4)	−0.0563 (6)	0.2642 (4)	0.0591 (3)	0.034
C(5)	0.0402 (5)	0.1866 (4)	0.0475 (3)	0.038
C(6)	0.0016 (7)	0.1198 (5)	−0.0225 (3)	0.060
C(7)	0.2599 (5)	0.2467 (4)	0.2977 (4)	0.038
C(8)	0.2114 (5)	0.1888 (4)	0.3735 (3)	0.032
C(9)	0.3045 (5)	0.1159 (4)	0.4006 (4)	0.042
C(11)	−0.1351 (5)	0.4114 (4)	0.2532 (4)	0.038
C(12)	−0.1443 (6)	0.3729 (4)	0.1613 (4)	0.040
C(21)	0.0802 (6)	0.3826 (5)	0.1284 (4)	0.041
C(22)	0.1944 (6)	0.3442 (5)	0.1771 (4)	0.042
C(31)	0.1286 (6)	0.3886 (4)	0.3223 (4)	0.043
C(32)	0.0070 (6)	0.3727 (4)	0.3706 (3)	0.039
H(01)	−0.22680	0.15306	0.21208	0.050
H(02)	0.13198	0.10700	0.11040	0.050
H(03)	0.03317	0.13066	0.39671	0.050

[a] $U_{eq} = {}^1/_3\sum_i\sum_j U_{ij}a_i^*a_j^*\mathbf{a}_i\cdot\mathbf{a}_j$.

Table III. Selected Bond Lengths (Å) and Bond Angles (deg) for the Complex $[MnLH_3][MnCl_4]$ (1)

Mn(1)–N(1)	2.253 (5)	Mn(1)–N(2)	2.240 (5)
Mn(1)–N(3)	2.241 (5)	Mn(1)–O(1)	2.149 (4)
Mn(1)–O(2)	2.167 (4)	Mn(1)–O(3)	2.181 (4)
O(1)–H(1)	0.984 (4)	O(2)–H(2)	1.030 (4)
O(3)–H(3)	1.085 (4)		
N(1)–Mn(1)–N(2)	79.1 (2)	N(1)–Mn(1)–N(3)	79.0 (2)
N(2)–Mn(1)–N(3)	79.9 (2)	O(1)–Mn(1)–O(2)	101.4 (2)
O(1)–Mn(1)–O(3)	98.5 (2)	O(2)–Mn(1)–O(3)	102.0 (2)
N(1)–Mn(1)–O(1)	78.6 (2)	N(2)–Mn(1)–O(2)	77.4 (2)
N(3)–Mn(1)–O(3)	77.6 (2)		

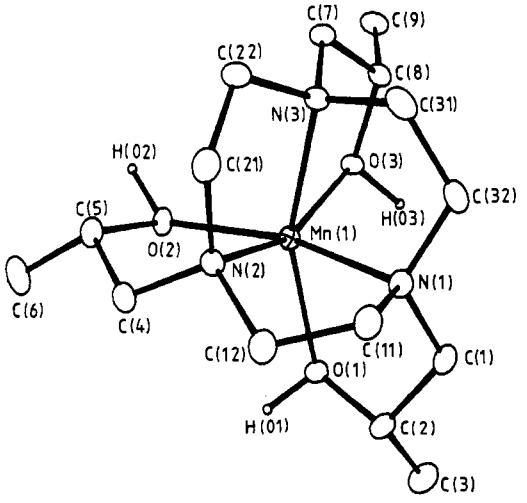

Figure 1. Molecular structure of the complex cation $[MnLH_3]^{2+}$ (cation of **1**) showing the atom-numbering scheme. Thermal ellipsoids represent 20% probability. Hydrogen atoms are represented by arbitrary spheres.

Crystal Structures of $[MnLH_3][MnCl_4]$ (1), $[MnLH_3LMn][PF_6]_3$ (2), and $[MnL'][ClO_4]$ (3). The crystal structure of **1** consists of

Table IV. Final Positional Parameters (Fractional Coordinates) with Esd's in Parentheses and Isotropic Thermal Parameters (Å²) (Equivalent Isotropic Parameters Used for Anisotropic Atoms) for $[MnLH_3LMn][PF_6]_3$ (2)

atom	x/a	y/b	z/c	U_{eq}[a]
Mn(1)	0.00000	0.00000	0.00000	0.026
Mn(2)	0.00000	0.00000	−0.12703 (4)	0.028
P(1)	0.00000	0.00000	−0.81689 (7)	0.039
P(2)	0.00000	0.00000	−0.30435 (8)	0.050
P(3)	0.00000	0.00000	−0.55426 (8)	0.051
F(1A)	0.1137 (5)	0.1335 (5)	−0.8425 (1)	0.064
F(1B)	−0.0207 (6)	0.1124 (6)	−0.7922 (1)	0.091
F(2A)	−0.0263 (10)	0.1044 (8)	−0.2780 (2)	0.131
F(2B)	−0.1357 (7)	−0.0345 (9)	−0.3295 (2)	0.135
F(3A)	0.0000	0.0000	−0.5118 (3)	0.136
F(3B)	0.0000	0.0000	−0.5968 (3)	0.162
F(3C)	0.01995	0.17081	−0.55493	0.152
F(3D)	−0.11879	0.04396	−0.55493	0.203
F(3E)	0.11423	0.16973	−0.55493	0.096
F(3F)	−0.06796	0.10599	−0.55493	0.208
N(1)	0.0589 (5)	0.1782 (5)	0.0419 (1)	0.034
N(2)	−0.0632 (5)	0.1104 (5)	−0.1623 (1)	0.040
O(1)	0.0636 (4)	0.1921 (4)	−0.0327 (1)	0.035
O(2)	0.1345 (3)	0.1655 (3)	−0.1011 (1)	0.029
C(10)	0.1905 (6)	−0.1425 (6)	−0.0148 (2)	0.042
C(11)	0.0736 (6)	0.3117 (6)	0.0230 (2)	0.042
C(12)	0.0032 (7)	−0.2001 (7)	0.0565 (2)	0.049
C(13)	0.1886 (7)	0.0621 (8)	0.0702 (2)	0.053
C(20)	−0.2393 (6)	0.0476 (7)	−0.1134 (2)	0.043
C(21)	−0.1352 (7)	0.1688 (6)	−0.1379 (2)	0.047
C(22)	0.0741 (8)	0.2295 (7)	−0.1791 (2)	0.052
C(23)	−0.1696 (8)	0.0018 (8)	−0.1906 (2)	0.054
C(100)	0.1299 (8)	0.4484 (7)	−0.0360 (2)	0.056
C(200)	−0.2864 (8)	0.1031 (9)	−0.0812 (2)	0.067
H(1)	0.06730	0.19620	−0.05740	0.050

[a] $U_{eq} = {}^1/_3\sum_i\sum_j U_{ij}a_i^*a_j^*\mathbf{a}_i\cdot\mathbf{a}_j$.

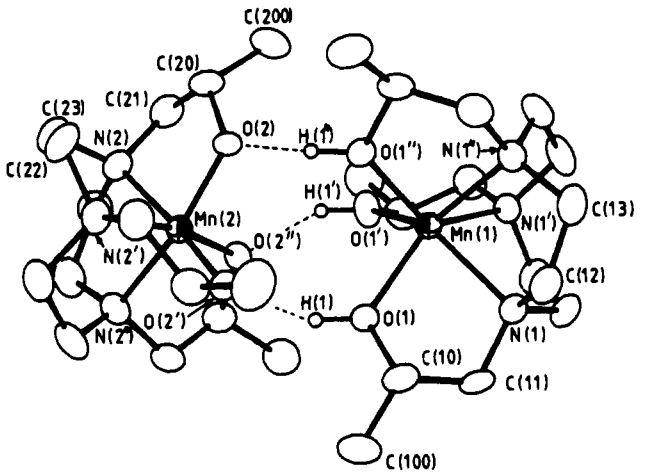

Figure 2. Molecular structure of the complex cation $[MnLH_3LMn]^{3+}$ (cation of **2**) showing the atom-numbering scheme. Thermal ellipsoids represent 20% probability. Hydrogen atoms are represented by arbitrary spheres.

$[MnL]^{2+}$ cations and $[MnCl_4]^{2-}$ anions, which are connected by hydrogen bonds. The cation is monomeric (Figure 1; Tables II and III), in contrast to both **2** and $[CoLH_3LCo]^{3+}$, and the ligand is fully protonated. Selected bond distances and angles are given Table III. The Mn–N and Mn–O distances are typical of Mn(II) complexes. The molecule is approximately halfway between octahedral and trigonal-prismatic geometry, having a twist angle of 37.4° (Table VIII). The three endocyclic chelate rings (in the tacn part of the ligand) have the λ conformation while the three exocyclic rings (formed by the arms) are in the δ conformation. The molecule has the overall absolute configuration Δ (λδ), which is the same as that adopted by both halves of $[CoLH_3LCo]^{3+}$ and by the Mn(IV) half of **2** (vide infra).

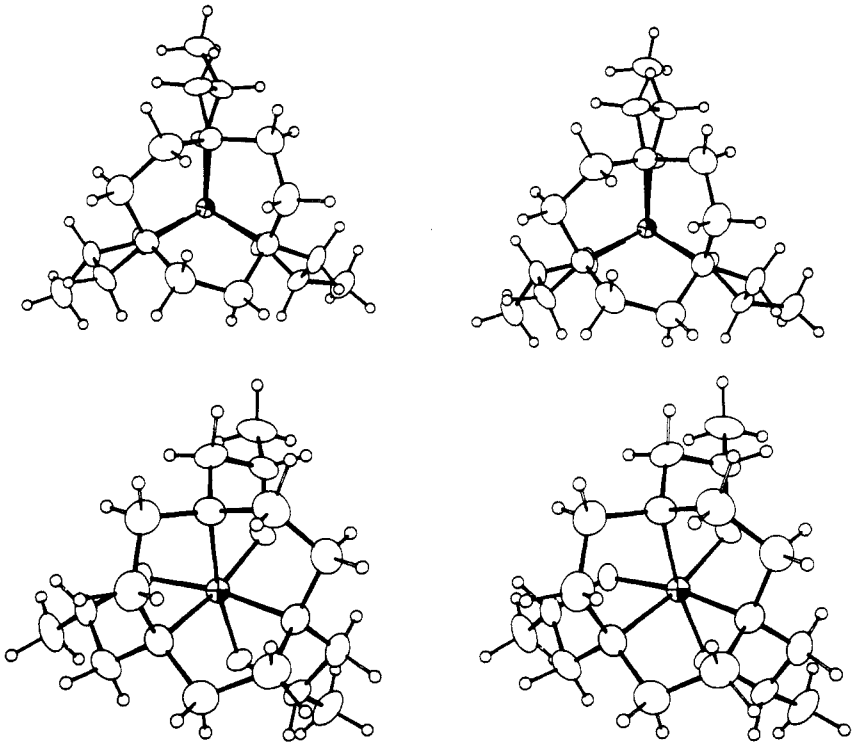

Figure 3. Stereoviews of each half of **2**, each looking down the trigonal axis. The top view is of the trigonal prismatic $[MnLH_3]^{2+}$ unit; the bottom view is of the pseudooctahedral $[MnL]^{+}$ unit.

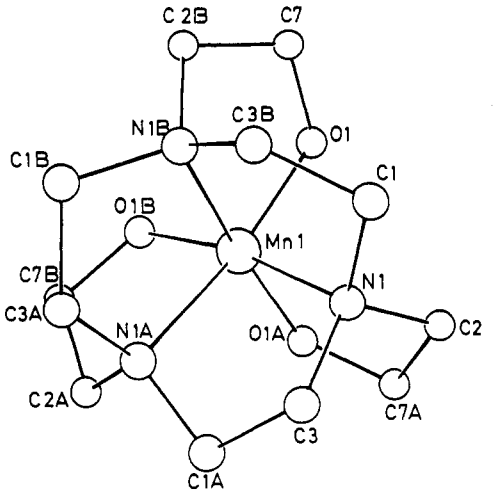

Figure 4. Molecular structure of the complex cation $[MnL']^{+}$ (cation of **3**) showing the atom-numbering scheme.

The crystal structure of **2** (Figure 2, Tables IV and V) has several interesting features. First, it is a dimer (like the Co(III) complex but unlike **1**). Unlike $[CoLH_3LCo]^{3+}$, however, the halves of the dimer have different geometries. This is shown more clearly in Figure 3 where stereoviews of the halves of the molecule are pictured looking down the Mn–Mn axis. The trigonal half of the dimer has Mn–N and Mn–O bond lengths which are similar to those of **1** (Table VIII). Because of this and of the chemical evidence mentioned above, this half of the dimer is identified as a Mn(II) complex, $[Mn^{II}LH_3]^{2+}$. The other half of the dimer has close to octahedral geometry and has Mn–N and Mn–O bond lengths which are almost identical to those of **3** and are close to those of $[CoLH_3LCo]^{3+}$ (Table VIII). This, taken with the electronic spectrum (and color) of the molecule and its magnetic moment, let us identify this half of the dimer as a Mn(IV) complex.

Both halves of the dimer have the same δ conformation for the exocyclic rings formed by the hydroxypropyl arms. The chelate rings formed by the tacn part of the molecule have, however, opposite conformations in each half. In the Mn(IV) half, as in $[CoLH_3LCo]^{3+}$, the rings are λ while in the Mn(II) half they have the δ conformation.

The Mn(IV) monomer, **3**, has a structure (Figure 4, Tables VI and VII) which is very similar to that of the Mn(IV) half of

Table V. Selected Bond Lengths (Å) and Bond Angles (deg) for the Complex $[MnLH_3LMn][PF_6]_3$ (**2**)

Mn(1)–N(1)	2.251 (5)	Mn(2)–N(2)	2.051 (5)
Mn(1)–O(1)	2.142 (4)	Mn(2)–O(2)	1.857 (4)
N(1)–C(11)	1.498 (7)	N(2)–C(21)	1.484 (8)
C(10)–C(11)	1.524 (8)	C(20)–C(21)	1.492 (9)
O(1)–C(10)	1.438 (7)	O(2)–C(20)	1.453 (7)
C(10)–C(100)	1.497 (10)	C(20)–C(200)	1.503 (10)
N(1)–C(12)	1.468 (8)	N(2)–C(22)	1.486 (9)
C(12)–C(13)	1.507 (9)	C(22)–C(23)	1.499 (10)
N(1)–C(13)	1.511 (8)	N(2)–C(23)	1.530 (9)
O(1)–H(1)	0.906 (4)	O(2)–H(1)	1.841 (3)
N(1)–Mn(1)–N(1)′	78.6 (2)	N(2)–Mn(2)–N(2)′	84.5 (2)
O(1)–Mn(1)–O(1)′	91.8 (2)	O(2)–Mn(2)–O(2)′	96.2 (2)
N(1)–Mn(1)–O(1)	77.0 (2)	N(2)–Mn(2)–O(2)	96.0 (2)

Table VI. Atomic Coordinates ($\times 10^4$) for $[MnL'][ClO_4]$ (**3**)

atom	*x/a*	*y/b*	*z/c*	occupancy
Mn(1)	2971.1 (6)	2971.1 (6)	2971.1 (6)	1.0
Mn(2)	523.5 (6)	523.5 (6)	523.5 (6)	1.0
Cl(1)	5352 (1)	5352 (1)	5352 (1)	1.0
Cl(2)	7817 (1)	7817 (1)	7817 (1)	1.0
N(1)	2933 (3)	4346 (3)	3141 (3)	1.0
N(2)	−1541 (3)	6394 (4)	4822 (4)	1.0
O(1)	1768 (2)	2801 (3)	3247 (3)	1.0
O(2)	321 (3)	6051 (3)	5218 (3)	1.0
C(1)	2571 (4)	4512 (4)	4083 (5)	1.0
C(2)	2288 (4)	4645 (4)	2414 (4)	1.0
C(3)	3875 (4)	4723 (4)	3034 (5)	1.0
C(4)	−1190 (4)	7333 (4)	4696 (5)	1.0
C(5)	−2377 (4)	6228 (5)	4262 (5)	1.0
C(6)	−1690 (5)	6188 (4)	5816 (4)	1.0
C(7)	1564 (4)	2574 (5)	4164 (4)	1.0
C(8)	1725 (5)	164 (4)	−902 (5)	1.0
O(11)	5903 (3)	5903 (3)	5903 (3)	1.0
O(12)	5245 (8)	5832 (7)	4521 (8)	0.5
O(13)	5087 (11)	4523 (12)	5743 (12)	0.5
O(21)	8385 (3)	8385 (3)	8385 (3)	1.0
O(22)	1894 (3)	1892 (3)	7090 (3)	1.0

Table VII. Selected Bond Lengths (Å) and Bond Angles (deg) for the Complex [MnL'][ClO_4] (3)

Mn(1)–N(1)	2.046 (5)	N(1)–C(1)	1.509 (8)
Mn(1)–O(1)	1.839 (4)	N(1)–C(2)	1.501 (8)
		N(1)–C(3)	1.506 (8)
Mn(2)–N(2)	2.041 (5)	N(2)–C(4)	1.491 (8)
Mn(2)–O(2)	1.833 (5)	N(2)–C(5)	1.505 (9)
		N(2)–C(6)	1.514 (8)
O(1)–C(7)	1.427 (7)		
O(2)–C(8)	1.431 (8)	C(1)–C(3A)	1.498 (10)
		C(4)–C(5A)	1.52 (1)
		C(6)–C(8A)	1.518 (9)
		C(2)–C(7A)	1.502 (9)

N(1)–Mn(1)–N(1A)	84.8 (3)	N2(A)–Mn(2)–N(2B)	83.0 (3)
N(1)–Mn(1)–O(1B)	168.7 (2)	N(2B)–Mn(2)–O(2A)	83.9 (3)
N(1A)–Mn(1)–O(1B)	83.9 (2)	O(2A)–Mn(2)–O(2B)	97.8 (3)
O(1)–Mn(1)–O(1A)	96.4 (3)	N(2A)–Mn(2)–O(2B)	166.7 (2)
N(1)–Mn(1)–O(1)	94.7 (3)	N(2A)–Mn(2)–O(2A)	94.8 (3)

Table VIII. Comparison of Selected Geometric Parameters for 1–3 and Related Molecules

complex	M–N, Å	M–O, Å	ϕ, deg[a]	ref
1	2.245[b]	2.166[b]	37.4	this work
2 (Mn(II) half)	2.251	2.142	60.0	this work
2 (Mn(IV) half)	2.051	1.857	10.9	this work
3	2.044[b]	1.836[b]	9.4[b]	this work
$[CoLH_3LCo]^{3+}$[c]	1.944	1.939	10.2	11
$[NiLH_3]^{2+}$	2.064	2.083	17.5	24
octahedron			0	
trigonal prism			60	

[a] ϕ is defined as the angle of twist of the two sets of ligators, looking down the C_3 axis, away from octahedral geometry. [b] Average value(s). [c] Deprotonated half of the dimer.

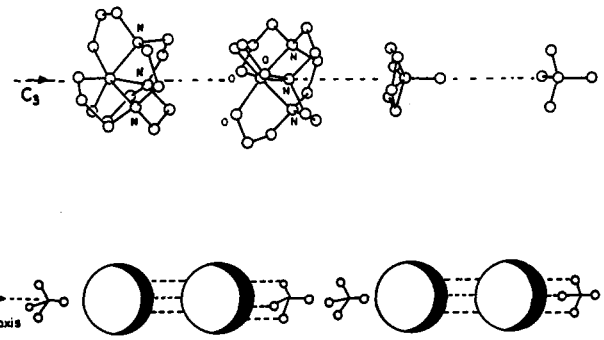

Figure 5. (a) Packing of the cations and anions along a crystallographic 3-fold axis of symmetry in crystals of [MnL'][ClO_4] (3). (b) Schematic representation of the same packing. Large spheres represent cationic complexes with the shaded areas representing the methylene groups of the ligand. The dotted lines represent possible C–H···O contacts.

2. Bond lengths and angles are almost identical as is the twist away from octahedral geometry (Table VIII). The crystal packing of 3 is of interest. The eight molecules in the unit cell are arranged in pairs (Figure 5) in which the alkoxy oxygens of one crystallographically independent molecule make weak contacts with three of the methylene hydrogen atoms of the second molecule. This pseudo "dimer" is flanked by $[ClO_4]^-$ ions, one of which forms weak hydrogen bonds to the methylene hydrogens of the $[ML']^+$ unit and is consequently disordered and one of which points toward the alkoxy atoms of the other $[ML']^+$ ion.

In both Mn(IV) complexes the Mn–N and Mn–O bond lengths are significantly different, the Mn–O bond length being shorter by approximately 0.2 Å. In the Co(III), Co(III) dimer[11] and in the Ni(II) complex,[24] in contrast, the M–N and M–O bond lengths are essentially identical. The Mn(II) complexes are intermediate, having a difference between the Mn–N and Mn–O bond lengths which averages 0.1 Å. We ascribe the difference to the π *bonding* interaction between the filled π orbitals on the oxygens and the partially empty t_{2g} set on the Mn(IV) or Mn(II) metal ions. Such bonding is not possible in the Co(III) and Ni(II) complexes since these have filled (t_{2g}^6) sets.

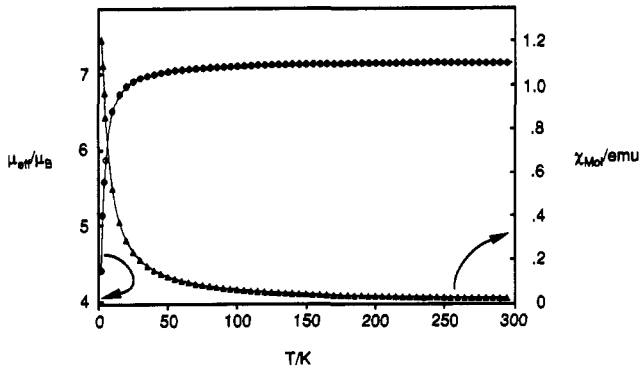

Figure 6. Plot of the magnetic moment, μ_{eff}/μ_B, and the magnetic susceptibility, χ_{mol}/emu, against temperature for **2**.

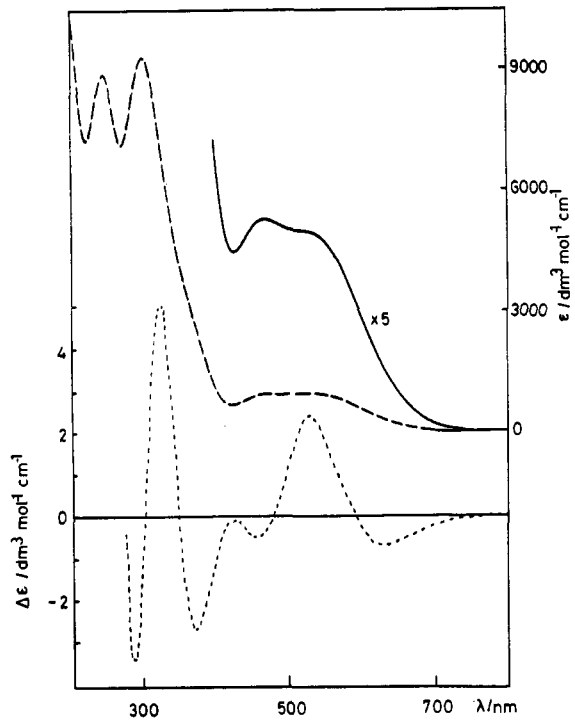

Figure 7. Absorption (upper curves) and CD spectra of **2** in MeCN solution.

Temperature-Dependent Magnetic Susceptibility of 2. The magnetic susceptibility of **2** as a function of temperature, T, is shown in Figure 6. The magnetic moment, μ/μ_B, decreases from 7.1 μ_B at 295 K to 4.4 μ_B at 2.0 K. This behavior is indicative of an intramolecular antiferromagnetic spin coupling. For a magnetically uncoupled Mn(II), Mn(IV) complex a magnetic moment of 7.07 μ_B is calculated ($((\mu_1^2 + \mu_2^2)^{1/2})$ whereas for a fully antiparallely coupled species ($S = 1$ ground state) a μ_{eff} value of 2.83 μ_B is calculated, which is not reached at 2 K. The Heisenberg–Dirac–van Vleck model for magnetic coupling in a dinuclear complex was used to interpret the temperature dependence of the magnetism. The data were fitted using a susceptibility expression derived from the spin–exchange Hamiltonian, $H = -2JS_1 \cdot S_2$ ($S_1 = {}^5/_2$, $S_2 = {}^3/_2$), where J is the spin-exchange coupling constant. The best least-squares fit for **2** gave $J = -0.66$ cm^{-1} and $g = 2.06$. No additional terms for temperature-independent paramagnetism or for a mole percentage of paramagnetic impurity were found to be necessary to obtain an excellent fit to the data.

The small antiferromagnetic coupling constant of **2** falls nicely within the range found for a number of dinuclear Cr(III) complexes where the monomeric units are connected by one, two or three $[H_3O_2]$–bridges.[25]

(24) Farrugia, L. J.; Peacock, R. D. *Acta Crystallogr. Sect. C* **1991**, *C47*, 1312.

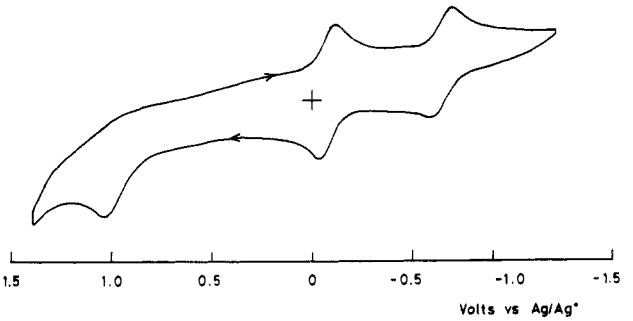

Figure 8. Cyclic voltammogram of **2** in MeCN solution. The reference is Ag/Ag^+ (0.1 mol L^{-1} $AgNO_3$ in MeCN).

Electronic and Circular Dichroism Spectra of 2. The absorption and CD spectra of **2** are shown in Figure 7. The absorption must all derive from the Mn(IV) part of the dimer since the Mn(II) unit will have only spin-forbidden transitions; confirmation for this comes from the fact that the absorption exactly doubles when the complex is basified with Et_3N and allowed to air oxidize. The absorption spectrum divides into two areas: two high-intensity bands ($\epsilon \sim 9000$ L mol^{-1} cm^{-1}) and a shoulder at higher energy, which are unambiguously assigned as charge-transfer bands, and two lower intensity bands ($\epsilon \sim 1000$ L mol^{-1} cm^{-1}) at lower energy. The visible spectrum of **3** is very similar (λ_{max}, nm (ϵ, L mol^{-1} cm^{-1}): 474 (850), 556 (750)). The intensities of the two low-energy bands are such that either a charge-transfer or a d → d assignment must be considered. The d^3 configuration gives rise to two spin-allowed ($^4A_{2g} \rightarrow {}^4T_{2g}$ and $^4A_{2g} \rightarrow {}^4T_{1g}$) transitions and a spin-forbidden $^4A_{2g} \rightarrow {}^2E_g$ transition in the visible region. The lowest spin-allowed transition ($^4A_{2g} \rightarrow {}^4T_{2g}$) of the analogous Cr(III) complex, $[CrLH_3Cr]^{3+}$, comes at 540 nm.[26] The Co(III),[11] Cr(III),[26] and Ni(II)[26] complexes of LH_3 all have "normal" intensity d → d transitions (ie ϵ's on the order of 10 for the nickel complex and on the order of 200 for the Co(III) and Cr(III) complexes). It is very difficult to see why the Mn(IV) complex should have d → d transitions with extinction coefficients of around 1000. More conclusive are the values of the dissymmetry factors of the three low-energy CD bands (5.0×10^{-4}, 2.5×10^{-3}, and 1.0×10^{-3}). The $^4A_{2g} \rightarrow {}^4T_{2g}$ transition is magnetic dipole allowed and so should have a dissymmetry factor on the order of 10^{-2}. The cobalt(III) and chromium(III) complexes of LH_3 have dissymmetry factors of 1.5×10^{-2} and 1×10^{-2}, respectively.[11,26] The dissymmetry factors of the CD bands of **2** are characteristic of electric dipole allowed–magnetic dipole forbidden bands rather than a magnetic dipole allowed d → d transition. We therefore assign the two low-energy absorption bands to charge-transfer transitions.

Cyclic Voltammetry of 2. The cyclic voltammogram of **2** in MeCN solution using platinum electrodes and an Ag/Ag^+ reference electrode is shown in Figure 8. There are two reductions: one at −0.06 V (0.54 V vs NHE) which is fully reversible and one at −0.64 V (−0.06 V vs NHE) which is quasi-reversible. An irreversible oxidation is observed at +1.07V (1.65 V vs NHE). The reversible reduction at −0.06 V must correspond to the process Mn(II), Mn(IV) → Mn(II), Mn(III) and the quasi-reversible reduction to Mn(II), Mn(III) → Mn(II), Mn(II). The irreversible oxidation must presumably be that for Mn(II), Mn(IV) → Mn(IV), Mn(IV). There is no obvious reason why such an oxidation should be *electrochemically* irreversible, but if the Mn(IV) species is a deprotonated monomer, the process would be *chemically* irreversible. The potentials are consistent with the Mn(II) species being oxidized to Mn(II), Mn(IV) by molecular oxygen.

Conclusions. The ligand LH_3 forms a Mn(II) complex $[MnLH_3]^{2+}$ (**1**) which is air stable in the solid state (and in solution provided the ligand cannot deprotonate). Under mildly basic conditions (water at pH 7 is sufficient), every second mole of ligand deprotonates, and aerial oxidation occurs to produce the mixed-valence dimer $[Mn^{II}LH_3LMn^{IV}]^{3+}$ (**2**). Addition of strong base, such as Et_3N, to a solution of **2** results in further oxidation to a Mn(IV) species which is presumably $[MnL]^+$. The analogous ion, $[MnL']^+$, can be produced directly as the $[ClO_4]^-$ salt by oxidation of a solution of $Mn(ClO_4)_2$ and $L'H_3$ with H_2O_2 or by oxidation of a solution of "manganese(III) acetate" and $L'H_3$ in air.

In **1**, the Mn(II) ion is pseudooctahedral with a trigonal twist of 37° whereas in **2** it is has exactly trigonal-prismatic geometry. When the metal ion shows an electronic preference for octahedral geometry (Co(III), Mn(IV), Ni(II)) the complexes have twist angles between 10 and 18°. It is tempting to suggest that the "natural" geometry for the Mn(II) complex with LH_3 is trigonal prismatic and that the distortion from this shown by $[MnLH_3][MnCl_4]$ is due to the extensive hydrogen bonding to the $[MnCl_4]^{2-}$ ions.

We suggest that the reason why a Mn(II), Mn(IV) species is formed instead of a Mn(III), Mn(III) one lies in the exacting stereochemical requirements of LH_3. Mn(III) has the $t_{2g}^3e_g$ electron configuration and so should be Jahn–Teller distorted. It would be extremely difficult for LH_3 (or $L'H_3$) to give the required tetragonal distortion, and it seems that this must be the driving force behind the stabilization of the relatively unusual Mn(IV) oxidation state in **2** and **3**.

Acknowledgment. We thank the University of Glasgow for a scholarship to I.F. and the Egyptian government for a Channel Studentship to A.A.B.

Registry No. **1**, 136657-67-5; **2**, 134588-30-0; **3**, 136599-85-4; $[MnLH_3]^{2+}$, 134588-29-7; [MnL], 134588-31-1.

Supplementary Material Available: Complete listings of crystallographic data (Tables S1 and S2), bond lengths and angles, anisotropic thermal parameters, and calculated hydrogen positional parameters (16 pages); listings of structure factors (33 pages). Ordering information is given on any current masthead page.

(25) Bossek, U.; Wieghardt, K.; Nuber, B.; Weiss, J. *Angew. Chem., Int. Ed. Engl.* **1990**, *29*, 1055.
(26) Macdonald, N. M. B.Sc. Thesis, 1990, University of Glasgow. Macdonald, N. M.; Peacock, R. D.; Robb, J. To be published.